Nature Climate Change Classification: Primary Research Article

Title: Quantifying global potential for coral evolutionary response to climate change

Authors: C.A. Logan[1]*, J.P. Dunne[2], J.S. Ryan[1], M.L. Baskett[3], S.D. Donner[4]

Address: 1 – Department of Marine Science, California State University, Monterey Bay, 100 Campus Dr., Seaside, CA 93955; 2 – NOAA/OAR Geophysical Fluid Dynamics Laboratory, 201 Forrestal Road, Princeton, NJ 08540; 3 – Department of Environmental Science and Policy, University of California Davis, Davis, California, 95616 United States of America, 4 – Department of Geography, University of British Columbia, 1984 West Mall, Vancouver, BC V6T 1Z2, Canada

Key Words: Climate change, coral, Symbiodiniaceae, shuffling, evolution, acidification, modeling

Author contributions: C.A.L., J.P.D., and S.D.D. conceived and designed the global model; C.A.L. and J.S.R. developed and tested the computer code; C.A.L., J.P.D., J.S.R. and S.D.D. analyzed the results; C.A.L. and J.S.R. wrote the paper. C.A.L., J.P.D., J.S.R., S.D.D., M.L.B. critically revised the manuscript.

Address correspondence to:
Cheryl A. Logan*; Email: clogan@csumb.edu

The authors declare no conflicts of interest

Abstract

Incorporating species' ability to adaptively respond to climate change is critical for robustly predicting persistence. We present the first global ecological and evolutionary model of competing branching and mounding coral morphotypes to examine the adaptive role of algal symbionts in setting coral thermal tolerance under global warming and ocean acidification. Symbiont shuffling (+1°C) was more effective than symbiont evolution in delaying coral cover declines with the largest differences occurring mid-century, but stronger warming rates associated with high-emissions scenarios outpace the ability of these adaptive processes and limit coral persistence. Acidification has a small impact on rates of reef degradation relative to warming rate. Global patterns in coral reef vulnerability to climate are sensitive to the interaction of warming rate and adaptive capacity, and cannot be predicted by either factor alone. Overall, our results show how models of spatially-resolved adaptive mechanisms can inform conservation decisions.

Introduction

Anthropogenic climate change is affecting marine ecosystems worldwide[1] and accelerating the rate of species extinctions[2,3]. Range shifts and rapid adaptation can circumvent this risk[4], but sessile species with low adaptive capacity are among those most threatened[5]. Incorporating adaptive capacity (e.g., due to genetics or acclimatization) into models of population size and geographic distribution can better predict climate change effects on species survival and ecosystem function[4,6,7].

Mechanistic predictions of adaptive capacity at a global scale can indicate where adaptation most affects future predictions[4,6]. Accounting for adaptive capacity might then shift expectations about overall vulnerability and where climate impacts might be greatest[8,9], which can inform conservation priorities[10]. For example, locations projected to experience greater future climate variability and extremes might be expected to also experience the greatest impacts. Yet species in these same locations might undergo selection for higher heat tolerance and therefore have greater adaptive capacity to warming. Given these contrasting possibilities, accounting for both evolutionary dynamics and climate stress can inform which locations might require more protection[9,11].

Coral reefs provide a model system for exploring interactions between adaptive capacity and vulnerability to climate stress. Corals are economically and ecologically important foundational species that have already experienced climate driven losses[12]. Under moderate emissions scenarios, global models suggest corals will experience bleaching more frequently than anticipated recovery rates by mid-century[13–15], though few have explicitly considered adaptive capacity (but see [16–20]). Compounding temperature-driven bleaching is ocean acidification (OA), which can impede coral skeletal growth, such that a challenge for predicting coral vulnerability is understanding the potential interactive effects of temperature and OA[15]. Coral growth and thermal tolerance are greatly affected by endosymbiotic photosynthetic microalgae[1] and symbiont-mediated adaptive capacity may enable corals to rapidly respond to warming. With large population sizes, high genetic diversity, and short generation times, symbionts have high adaptive potential[1–3] and shuffling towards more heat-tolerant taxa has been shown to increase bleaching thresholds by up to 1.5°C over ecological timescales[21,25]. Modeling natural adaptive processes is critical for making conservation decisions especially given human interventions being considered to increase coral heat tolerance[26,27].

Here, we quantitatively assess the effect of symbiont-mediated adaptive capacity using a global ecological and evolutionary model capable of simulating coral responses to warming and OA. Our model (Fig. S1) includes two ecologically realistic coral morphotypes[28] that compete for space: (1) a competitive, faster growing, heat-sensitive branching coral relative to a (2) slower growing, heat-tolerant mounding coral. We assume coral growth and thermal tolerance are an emergent property of symbiont population size and thermal characteristics [29]. Symbiont genotypes determine thermal optima, while the coral host determines sensitivity to temperature departures from that optimum, with initial symbiont genotypes matched to local thermal history. We simulate symbiont-mediated adaptive capacity in both coral morphotypes through a) natural selection of symbiont populations (evolution[22–24]), and b) shifts between heat-sensitive and heat-tolerant symbiont communities ("shuffling"[21,25]). Evolution is simulated using a quantitative genetic model which results in thermal tolerance increases of 0.3-1.8°C depending on climate scenario and reef location. Shuffling is simulated by addition of a heat-tolerant symbiont population with a thermal growth optimum

+0.5, 1, or 1.5°C above that of a heat-sensitive symbiont population[21] that becomes competitively superior under warming. We also estimate potential effects of OA on coral growth based on changes in aragonite saturation[30]. We apply the model to projected monthly sea surface temperatures through 2100 in 1,925 reef cells to characterize regions where adaptive capacity most alters expectations about relative climate impacts.

Results

The global model supported coexistence of mounding and branching coral populations at steady-state between 1861 and 1950, prior to major anthropogenic warming, given our parameterization for interspecific competition. In simulations where the anthropogenic signal was removed, both morphotypes coexisted through 2300, regardless of starting proportions (Fig. 1; Fig. S2). At steady-state, branching corals comprised ~90% of total carrying capacity and mounding corals filled ~1%. To quantify changes in coral cover in simulations with and without adaptive capacity, we examined how relative coral extent varies through time. Relative coral extent is defined here as the percent of fixed pre-warming carrying capacity (K) made up by both coral morphotypes in each reef cell and averaged across all cells (weighted equally). Actual available coral habitat varies widely by reef so relative extent does not directly correlate to geographic extent.

In baseline model runs (i.e., no adaptive capacity), relative coral extent was ≤3% by 2100 under all climate scenarios except RCP 2.6 (37%) (Table 1). In these RCPs, most reef cells had experienced ≥2 bleaching events in the previous decade or were dead by 2050 (such reef cells hereafter are referred to as "degraded"; see *Methods*) reaching degradation rates >95% by 2100 (Fig. 1 and S3, black lines). We define bleaching as a decrease in symbiont density below 30% of the minimum symbiont population size in the previous year (Fig. S4). Although end-of-century degradation rates were lower in RCP2.6 (43%), 98% of reef cells were comprised of only mounding corals, following a shift from branching to mounding communities in the 2040s across all RCPs (Fig 2, top row). Sensitivity analyses shows that coral persistence is enhanced if the model is normalized to a lower 1985-2010 global bleaching frequency but that relative differences among adaptive mechanisms remain the same (Fig. S5).

Effects of Symbiont-Mediated Adaptive Capacity

Shuffling (+1°C advantage) significantly delayed or prevented widespread mortality by 2100, with the largest differences in RCP4.5 and RCP6.0 (Table 1). Relative coral extent at 2100 increased dramatically in RCP4.5 (3 to 28%) and branching coral populations increased from 0 to 18% in relative coral extent across most reef cells. In RCP2.6, shuffling averted mid-century population declines and a shift towards mounding coral communities (Fig. 2). In contrast, shuffling had little effect in RCP6.0 and RCP8.5 by 2100 (Table 1), with relative coral extent remaining ≤5%. Shuffling (+1.5°C advantage) increased relative coral extent to 58% for RCP6.0, but remained ≤3% for RCP8.5 (Table S1). Shuffling (+0.5°C advantage) had little effect on relative coral extent at 2100 (≤2% for all RCPs except RCP2.6) (Table S1). Fidelity to heat-tolerant symbionts occurred in both coral morphotypes between 2010-2025 in most reef cells, maximizing thermal tolerance by 2040 (Fig. S6). A complete transition to heat-tolerant symbiont communities occurred in under 5-10 years on some reefs (Fig. S7).

Evolution also delayed degradation most under RCP4.5 and RCP6.0, but had little effect on relative coral extent under RCP 8.5 (Figs 1 & 2). Relative coral extent increased most under

RCP4.5, from 3 to 41% by 2100 (Table 1) and degradation was delayed by ~50 years (Fig. 1b, blue vs black lines). By 2100, mounding coral populations became dominant in most reef cells (Fig. 2). Under RCP2.6, evolution increased relative coral extent from 37 to 81% (Table 1) and branching corals remained dominant in most reef cells by 2100, albeit with large mid-century population declines (Fig. 2, third row). Compared with shuffling (+1°C), evolution was slightly more effective in averting decline of coral populations in RCP2.6 initially, but less effective by mid-century under all RCPs (Fig. 1 & 2; Table 1).

In model runs where shuffling (+1°C) and evolution occurred concurrently, coral persistence dramatically increased in RCP4.5, RCP6.0, and RCP8.5 (Fig. 1). These simulations show similar trends to shuffling-only during mid-century, but evolution continues to increase thermal tolerance through 2100. Relative coral extent was ≥58% by 2100 in all RCPs except RCP8.5 where it remained 10% (Table 1). Only simulations where both shuffling (+1.5°C) and evolution co-occur enabled moderate coral persistence by 2100 under RCP8.5 (47% relative coral extent) (Table S1).

To examine how adaptive capacity altered expectations for relative vulnerability across locations, we compared the last year in which reef cells avoided degradation under RCP4.5 and RCP8.5 (Fig. 3). In the baseline model, degradation occurred earliest in the Red Sea, the Persian Gulf, and the western equatorial Pacific (Fig. 3a,b). Coral persistence was higher in the central Pacific, and near Malaysia and western Indonesia. Shuffling (+1°C) slowed rates of degradation in the central Pacific and Coral Triangle under RCP8.5 (Fig. 3d,b), areas with both lower projected warming and SST variability (Fig. S9b,j). Under RCP4.5, shuffling had a stronger global effect compared to baseline, except in high latitude areas with higher seasonal variability (e.g., northern Red Sea, East China Sea) and locations projected to have high interannual maximum SST variability (e.g., southern Caribbean, equatorial Pacific) (Fig. S9e,f). Evolution showed similar geographic patterns as for shuffling under RCP4.5. Exceptions include parts of the Caribbean, where evolution only increased persistence near the Greater Antilles (Fig. 3e) in relation with relatively lower projected warming (S9a,b) and SST variability (S9i,j). Under RCP8.5, evolution had a small effect compared with baseline model runs (Fig. 3f,b) with no apparent refugia emerging, although global degradation rates were delayed ~5-10 years. In simulations with combined evolution and shuffling (+1°C), most reef cells within the Coral Triangle and central Pacific survived through 2080 under RCP4.5 and RCP8.5 (Fig. 3g,h).

To evaluate environmental predictors of modeled extinction risk, we compared model vulnerability maps (Fig. 3) to global maps of warming rate and SST standard deviation (Fig. S9), but none were consistent indicators of vulnerability across locations. Correlations were highest between relative coral extent and future SST variation (all months) in shuffling runs, with R^2 ranging from 0.41 to 0.55; all other SST metrics and simulations had average R^2 values < 0.2 (Table S4).

Effects of Ocean Acidification

In simulations where OA negatively affected coral growth, coral degradation was greater across all reef cells, but not by more than 5% in any year (Fig. S5). This effect was greatest when warming drove moderate reef mortality. For example, in RCP8.5, OA increased percent of degraded reefs from 55.7% to 58.6% by 2050. Prior to 2020 when many reefs were still healthy and after 2070 when mortality was high, OA had little effect on growth rate.

Discussion

Our results demonstrate that incorporating species' ability to adaptively respond to climate change is critical for robust, global-scale predictions of species' future persistence and extent. Model simulations without adaptation predicted coral persistence through 2100 only under RCP2.6 (Fig. 1-2), similar to previous threshold-based global-scale bleaching models[13–15]. Symbiont-mediated adaptive capacity significantly altered coral population trajectories under low and moderate warming scenarios, but had little effect under RCP8.5. Shuffling was generally more effective than evolution in delaying coral cover declines and shifts towards mounding coral communities (Figs. 1-2). Under RCP8.5, the only simulation with >1% of "healthy" reef cells by 2100 included both symbiont evolution and shuffling, resulting in a relative coral extent of 10% (Table 1).

These results expand upon previous studies[17,19] to demonstrate how adaptive mechanisms can increase coral persistence under low to moderate but not severe climate change. We found that when shuffling provided +1°C thermal advantage, coral persistence increased more than with evolution alone (Fig. 2). Evolution enabled most reef cells to persist through 2100 under RCP2.6 (Fig. 1-2) but was slightly less effective at increasing persistence than shuffling with a +1°C advantage as the more rapid shuffling mechanism has its largest impact between 2010 and 2040 (Fig. 2 & S6) whereas evolution occurs at a slower rate but over a longer duration (Fig. 2 and S8). Under RCP8.5, adaptation delayed complete coral mortality by less than a decade but did not significantly change century-scale outcomes. Symbiont-mediated adaptive processes acting concurrently substantially prolonged coral survival under RCP4.5 and RCP6.0 with minimal shifts in coral community composition (Table 1; Fig. 1).

Coral community shifts described here have been reported in the field following bleaching events[31] but have not previously been globally projected. From an ecological perspective, community shifts are likely to compromise reef structural complexity and long-term stability of reef-associated biodiversity[32]. We found that shifts towards mounding coral communities began earlier with evolution than with shuffling (Fig. 2), further demonstrating how these mechanisms result in different outcomes. Shuffling maximizes thermal tolerance in most reefs by 2040 after which time both coral morphotypes exhibit fidelity to heat-tolerant symbionts (Fig. S6), as has been observed in some of the hottest reefs in the world[33]. We also identified scenarios where adaptive capacity enabled coral communities to shift back to baseline when warming rates declined (e.g., RCP2.6 with evolution; Fig. 2). Though this trajectory would only be possible under conditions not fully considered in our model (i.e., adequate recruitment, available substrate, and reduction of local stressors), it suggests adaptive mechanisms may enable some reefs to retain present-day structure and function under RCP2.6.

Previous work has suggested only a minor additional impact of ocean acidification (OA) on coral persistence compared with warming[14] with benefits of higher latitude thermal refugia largely offset by relatively lower aragonite saturation (Ω) values[15]. Our results suggest an even lower OA sensitivity with an attributable global reduction of coral persistence to OA of <5% (Fig. S5). This agreement suggests that effects of OA through Ω-reduced bleaching thresholds and Ω-reduced growth rates are minor compared to warming. However, modeling including substrate strength effects found a 70% drop in coral cover with a doubling of atmospheric CO_2[34]. Thus, OA influences through Ω effects on bleaching susceptibility and substrate strength may play a much more important role than through the growth rate mechanism in the present study.

Our model identifies regions where adaptation alters expectations about where climate impacts are highest. In some cases, we found that relative vulnerability was similar with and without adaptation. For example, higher latitude reef cells with higher seasonal variability were among the most vulnerable locations regardless of adaptation under RCP4.5 (Fig. 3; left panels). Yet, in other regions, relative vulnerability differed when adaptive capacity was included. In the Coral Triangle, most reefs persisted through 2100 with adaptation in RCP4.5, whereas large portions were among the most vulnerable with no adaptation. Geographic patterns of persistence were somewhat similar between evolution and shuffling, with some key exceptions. For example, shuffling is projected to increase persistence across the entire Caribbean region under RCP4.5, whereas evolution only enabled long-term persistence in reef cells where both warming magnitude and SST variation is projected to be relatively lower (Fig. S9a,i). Under RCP8.5 (Fig. 3 right panels), evolution had little effect but shuffling enabled reefs in the central South Pacific and central Coral Triangle to persist 20-25 years in relation with relatively less projected warming and SST variability (Fig. S9b,j).

Given the threat to coral reefs even with <1.5°C of global warming[35], research is increasingly focusing on identifying conservation priorities. Overall, the results highlight that such research, typically based on current reef status and response to past disturbances[36], should include relative future warming and adaptive potential. For example, Walsworth et al. (2019) found that optimal management strategies focus on coral thermal refugia in models without adaptation, but prioritizing trait and habitat diversity or high cover is more effective in models with adaptation[11]. We also show that geographic patterns in model results depend on adaptive mechanism modeled (Fig. 3) and areas predicted to be more vulnerable based on change in SST or SST variation alone did not always predict vulnerability (Fig. S9). Other adaptive mechanisms not simulated here may produce different geographic patterns of persistence and vulnerability.

Like all models, our simplistic representation of coral reef ecology and evolution introduces several uncertainties and biases that might affect our results. Abiotic and biotic factors not included here might lead us to overestimate coral persistence and recovery, including light, sea level rise, storm damage, pollution, overfishing, herbivory, coral disease, and competition for space with other organisms[37]. Factors that might lead us to underestimate likelihood of persistence include other mechanisms of adaptation[38] (e.g., coral host adaptation/acclimatization or epigenetics), and explicit representation of gene flow[17,18,39]. In addition, while coarse resolution SSTs can capture average bleaching incidence across locations[40], bleaching incidence will further depend on local-scale factors such as high-frequency temperature variation and depth, which are potential mitigators of bleaching[41]. Climate model downscaling would be needed to inform local-scale management decisions. Furthermore, models with different climate sensitivity[42] and climate variability (e.g., ENSO) may give quantitatively different results. In addition, uncertain model parameters could lead to over- or underestimation of coral persistence. Selectional variance (symbiont thermal tolerance breadth) was the most sensitive parameter in a sensitivity analysis completed on a regional version of this model[19]. In our study, selectional variance was calibrated to reef cell thermal history and historical global bleaching frequencies. Future studies could include revised estimates of past bleaching events.

Our model also highlights research avenues that could improve our understanding of symbiont-mediated adaptive processes. First, the prevalence of shuffling across coral taxa in wild populations remains unclear. Although multiple symbiont types have been detected at low abundance in most coral taxa examined[43], not all corals have the flexibility to "shuffle"[33,44–46].

Second, the degree to which symbiont thermal tolerance can evolve and confer coral host tolerance in the wild is unknown. Heat-evolved Symbiodiniaceae lab strains have shown increased growth at temperatures 1-4°C above ambient temperatures after 40-120 generations, but these gains did not always increase coral heat tolerance[24,47]. Finally, more empirical measurements of time-dependent thermal performance curves[48] for both coral and symbiont growth would improve our ability to model population growth dynamics.

Due to recent increases in mass bleaching events worldwide[12], the management community is evaluating human interventions that may increase the persistence of coral reefs[26,27]. If the 2015 Paris Agreement upper goal of limiting warming to less than 2°C is reached, this would align mostly closely with RCP2.6. Under this scenario, symbiont-mediated increases in thermal tolerance might enable corals to survive through 2100 without drastic shifts in coral community composition. Under RCP4.5, evolution and shuffling could improve projections of coral cover and degradation rates. However, under RCP6.0 and 8.5, coral-dominated communities as we know them today are expected to essentially disappear. As managers and decision makers consider human interventions to increase thermal tolerance or decrease local thermal stress[26], assessing existing potential natural adaptive capacity using mechanistic models could help inform decisions[27].

Methods (online only)

We scaled and modified a coral-symbiont eco-evolutionary model originally described in Baskett et al. (2009) to the global level[19]. Here we provide a description of the model (Fig. S1) and modifications made to globalize the model and incorporate potential effects of ocean acidification.

Coral population dynamics and parameters. The model follows area cover for two coral morphotypes, a heat-tolerant slow-growing mounding type (C_M) and a heat-sensitive fast-growing branching type (C_B) (Fig S1, equations 1-6). These traits are generally based on those associated with common mounding and branching morphotypes, respectively[49]. Coral thermal tolerance depends on symbiont populations whose genotypes determine thermal optimum (see *Symbiont population dynamics* section below). Corals compete for space in a closed system using Lotka-Volterra dynamics with a competition factor α_{mn} (the competitive effect of coral *n* on coral *m*) and a fixed carrying capacity (K_{Cm}) that varies by coral type *m* (*M* or *B*). Branching corals are more competitive than mounding corals as in Langmead and Sheppard (2004)[50]. Carrying capacity was determined based on area occupied by each morphotype (to report coral cover in cm^2) and multiplied by a conversion constant from projected area to total surface area[51]. Coral growth rates decline linearly with increasing coral density to represent coral density dependence. Growth rates increase linearly with symbiont density (S_{im} relative to symbiont carrying capacity per unit of coral density K_{Sm}) to represent corals' dependence on symbionts for carbon[29,52], up to a coral-specific maximum growth rate of γ_m based on [53]. The model assumes that symbiont density is within a range such that increases in symbiont densities lead to increased coral carbon acquisition and growth[54,55]. Coral basal mortality rates are fixed (μ) in the absence of symbionts with parameters based on [51,56] and decrease as symbiont density increases. Mortality rates exceed growth rates when symbiont density is ~0.5×10^6 cell/cm^2 (a density where bleaching has been observed in the field[57]) and are represented in the model by u_m, the influence of symbiont density on coral mortality. In simulations with ocean acidification, we multiply coral growth by the coral calcification rate *f* (see *Ocean acidification* section below).

All coral parameters (K_{Cm}, α_{mn}, γ_m, μ_m, u_m) vary by coral type *m*, with branching corals (C_B) having a higher fixed carrying capacity (K_{Cm}), a greater competitive ability (α_{mn}), a faster growth rate (γ_m), higher basal mortality in the absence of symbionts (μ_m), and a lower value for the influence of symbionts on mortality (u_m) (Table S2 and references therein). Coral population dynamics are:

$$\frac{dC_m}{dt} = C_m \left[\frac{f^2 \gamma_m \frac{\sum_i S_{im}}{K_{Sm} C_m}}{K_{Cm}} \left(K_{Cm} - \sum_n \alpha_{mn} C_n \right) - \frac{\mu_m}{1 + u_m \frac{\sum_i S_{im}}{K_{Sm} C_m}} \right]. \qquad (1)$$

Symbiont population dynamics and parameters. We follow symbiont population size S_{im} as the number of cells of symbiont type *i* in coral type *m* (cells/cm^2 of coral) (Fig. S1, equation 2). Density dependence regulates symbiont density in each coral. Total symbiont carrying capacity per unit area, K_{Sm}, is proportional to C_m, the three-dimensional coral surface area and based on peak values for symbiont densities described in [57]. Symbiont carrying capacity is independent of genotype and scaled by the maximum symbiont population growth rate $\hat{r}(t)$ such that the symbiont type with the greater population growth rate, $r_{im}(t)$, is competitively superior. In other words, because we scale competition between symbiont types by growth rate, relative growth for a given

temperature determines the competitive outcome. The temperature-dependent maximum symbiont population growth rate function, $\hat{r}(t) = ae^{b\theta(t)}$, is based on the Eppley equation, where a and b are constants found for phytoplankton[58,59]. Symbiont population dynamics, S_{im}, of symbiont type i in coral type m are:

$$\frac{dS_{im}}{dt} = \frac{S_{im}}{K_{Sm}C_m}\left[r_{im}(t)K_{Sm}C_m - \hat{r}(t)\ \sum_j S_{jm}\right], \quad (2)$$

where S_{im} is number of cells for symbiont type i in coral type m. Symbiont populations grow based on the difference between their thermal tolerance phenotype and the temperature $\theta(t)$ (which varies with time t) according to a temperature-dependent exponential growth rate equation derived from phytoplankton[58] given parameters a and b. a was set such that the maximum symbiont growth rate is similar to the value reported [29] and b is from [59]. The width of this thermal tolerance function, thermal tolerance breadth σ^2_{wm}, depends on coral type m and is inversely related to selection strength in simulations with evolution. Thermal tolerance breadth varies by coral host to allow greater thermal tolerance (i.e., slower drop-off in growth with temperature departures from the symbiont-genotype-determined optimum) in mounding versus branching coral morphotypes (e.g., due to coral morphology or physiology) through differential susceptibility of each coral's symbionts to thermal stress. Symbiont populations have thermal tolerance phenotypes (temperature at peak performance) normally distributed around mean genotype $\bar{g}_{im}$ with environmental variance σ^2_e (described below). Thermal tolerance genotypes also follow a normal distribution with mean $\bar{g}_{im}(t)$ and variance $\sigma^2_{gim}(t)$, both of which are constant in simulations without evolution and vary in time for evolution model runs. The overall population growth rate $r_{im}(t)$for symbiont population i in coral host m is:

$$r_{im}(t) = \left\{1 - \frac{\sigma^2_{gim}(t)+\sigma^2_e+[\min(L,\bar{g}_{im}(t)-\theta(t))]^2}{2\sigma^2_{wm}}\right\} ae^{b[\theta(t)-2*\min(0,\theta(t)-\bar{g}_{im}(t)+L)]}. \quad (3)$$

Following this equation, symbiont growth rate ($r_{im}(t)$) decreases at temperatures higher or lower than the optimum, with steeper declines occurring at temperatures above the optimum for growth rate. This modified version of the equation from Baskett et al. (2009)[19] includes a minimum function so that a rapid drop in symbiont growth rate only applies when temperatures are higher than symbionts' adapted genotype, thus avoiding unrealistic cold water mortality events prior to the onset of 20th century warming. The minimum function varies with thermal tolerance breadth where $L = \sqrt{2.6\sigma^2_{wm}}$. Negative population growth rates indicate that mortality rate exceeds reproduction rate and can disrupt symbiosis and lead to bleaching. Symbiont populations have an initial mean thermal tolerance phenotype and genotype $\bar{g}_{im}(0)$ equal to mean historical sea surface temperature (SST) in each reef grid cell between 1861-2000. Thermal tolerance breadth σ^2_{wm} is proportional to variance in historical monthly SST between January 1861 and December 2001 and assumes that corals already living in more variable thermal environments have greater capacity to withstand larger thermal fluctuations.

Symbiont genetic dynamics. In evolution simulations, we model symbiont thermal tolerance as a haploid quantitative genetic trait using a continuous time approach. The "thermal tolerance phenotype" (described above) is the temperature to which a single symbiont population is adapted in each of the two coral morphotypes and based upon its mean population genotype. For each symbiont population *i* in coral *m*, the population genotype is modeled as a normal distribution with a mean genotype $\bar{g}_{im}$ and, for models with evolution, genetic variance of σ^2_{gim} (Fig. S1, equations 4 and 5). The phenotype varies around the genotype with random environmental variance σ^2_e (i.e., fraction of variation not due to heritability). Heritability (h^2) of thermal tolerance was estimated to be 0.330, an estimate for typical physiological traits[60]. Heritability estimates of coral thermal tolerance driven by symbionts, have been found to range between 0.23 to 0.5 . Environmental variance σ^2_e was calculated as the fraction of total phenotypic variation (σ^2_P) not explained by h^2 , such that σ^2_e = (1- h^2)*(σ^2_P). The mean genotype dynamics are:

$$\frac{d\bar{g}_{im}}{dt} = \frac{\sigma^2_{gim}(t)[\theta(t)-\bar{g}_{im}(t)]}{\sigma^2_{wm}} ae^{b\theta(t)} . \quad (4)$$

Within a population, genetic diversity can increase through new mutations and decrease through selection. In the model, mutation increases genetic variation a constant rate of σ^2_M. Mutational variance is calculated as $\sigma^2_M = \sigma^2_e$ x 0.001yr^{-1} as in Baskett et al. (2009)[19] and based on reported values for the ratio σ^2_M:σ^2_e as 0.0001–0.05 per generation for a variety of model organisms[61] and on the approximate symbiont generation time of 0.2 years[21]. The model assumes that stabilizing selection occurs for the optimal phenotype and is represented by selectional variance (σ^2_{wm}), or thermal tolerance breadth, which is inversely related to selection strength. Selectional variance is proportional to the width of the symbiont population growth rate (fitness) function. The genetic variance dynamics are:

$$\frac{d\sigma^2_{gim}}{dt} = \sigma^2_M - \frac{\sigma^4_{gim}(t)}{\sigma^2_{wm}} ae^{b\theta(t)} . \quad (5)$$

Values for all symbiont parameters (K_{Sm}, a, b, σ^2_e, σ^2_M, σ^2_{wm}) are based on Baskett et al. (2009)[19] and references therein (Table S2).

Finally, we set the selectional variance (σ^2_{wm}; width of the fitness function or thermal tolerance breadth) to be proportional to the historical mean and variance in each reef cell using a proportionality constant, ρ. In the absence of precise global bleaching records available to "tune" the model to each individual reef cell's bleaching history, we applied a heuristic approach at the global scale to define ρ. Similar to our previous study[16], we modified ρ to result in a global bleaching frequency of 3 or 5% between 1985-2010 (i.e., x% of the reef cells bleach, on average, in a given year). The accurate global bleaching frequency during this timeframe is not knowable, but these bleaching frequencies are within the range of realistic possibilities based upon extrapolation from a high-resolution global bleaching database and fall within the range of annual severe bleaching occurrences across 100 regions between 1985-2010[12].

The proportionality constant (ρ) was defined for each reef cell based on the ratio between the historical (1861-2000) mean and variance of the exponential term of Eppley's equation[58] ($e^{0.0633T}$) to capture physiological effects of temperature variability across time and space:

$$\rho = \frac{1}{s}\left[\frac{mean(e^{bT})}{var(e^{bT})}\right]^{y}.$$

Empirical values *s* and *y* remain constant across all reefs for any given RCP, but *s* varies with each adaptation simulation (e.g., baseline, shuffling, and evolution) to tune the global bleaching frequency to the historical bleaching target (see Table S3). The proportionality constant assumes a greater physiological effect of temperature variability at high than low temperatures; the physiological effects of temperature variability depending on the kinetics of activation energy which, for many organic reactions, follow the Eppley exponential curve[58]. We then constrain the proportionality constant to between 0.5 and 1.50 to best match to the targeted global bleaching frequency between 1985 and 2010. To determine selectional variance (σ_{wm}^2), or thermal tolerance breadth, the proportionality constant is then multiplied by the historical temperature variance in each cell. For mounding corals σ_{wm}^2 is then increased by 25% which provides a wider thermal tolerance range compared with branching (heat-sensitive) corals.

Symbiont "shuffling". To simulate the possibility of "shuffling" as a result of symbiont diversity, simulations begin with two symbiont populations in each coral type (evolution-only simulations include only one symbiont population). The additional population begins as a low abundance heat-tolerant symbiont type (e.g., genus *Durusdinium*). Heat-tolerant symbionts have an initial thermal optimum ($\bar{g}_{2m}$) of +0.5, 1, or 1.5°C above that of the heat-sensitive symbionts, enabling them to grow faster as temperature increases. The symbiont population growth rate (r_{im}) is calculated from the mean genotype $\bar{g}_{im}$, so the symbiont growth rates are different between the two symbiont types, with heat-tolerant symbionts having a higher maximum growth rate according to the Eppley function. Density dependence within and between symbiont populations regulates symbiont density in each coral morphotype at a level proportional to C_M given total symbiont carrying capacity per unit area K_{Sm}. Density dependence is scaled by the maximum possible population growth rate $\hat{r}(t)$ so that the symbiont type with the greater population growth rate $r_{im}(t)$ under a given temperature at time *t* is competitively superior. The model includes also a trade-off for hosting heat-tolerant symbionts where corals hosts are penalized with up to a 50% decrease in coral growth rate (similar to [63]). The growth penalty is proportional to the percent of heat-tolerant symbionts in each coral and applied by multiplying the coral growth rate (λ_m) by this weighted value after each time step. If temperature decreases, the heat-sensitive symbiont type can re-populate the coral, removing both the thermal advantage and the coral growth penalty. The goal was to simulate symbiont community shifts due to heat-tolerant symbionts being present in low abundance that could become dominant after bleaching[64]. Our model also assumes a trade-off between growth rate and thermal tolerance such that competition between the symbiont populations depends on temperature (i.e., the symbiont type with the greater population growth rate $r_{im}(t)$ is competitively superior). To test the effect of symbiont evolution in combination with shuffling, we also included model runs with and without evolution of both symbiont types.

Ocean acidification. To test the effect of ocean acidification on coral growth rate, we used a relationship between r and coral calcification rate (f) previously described[30], where a 0.15 slope represents the mean sensitivity of coral calcification to Ω_{Arag} across multiple coral taxa:

$$f(\Omega_{Arag}) = 1 - 0.15(4 - \Omega_{Arag}) \quad where \quad 1 \leq \Omega_{Arag} \leq 4\,. \qquad (6)$$

Based on equation 6, Ω_{Arag} values were calculated for each reef cell for all four RCPs (NOAA-GFDL ESM2M[65,66]). For Ω_{Arag} values below one the factor is set to zero, and for values above four the factor is set to one. For ocean acidification model runs, this function was included in the equation for the coral growth rate (equation 1). The value of f is squared because calcification rate correlates with linear growth rates[67], but coral population size is estimated from total coral surface area calculated in two dimensions.

Model application. The model applies differential equations (Fig. S1) for coral and symbiont growth, competition, and genetic adaptation of symbionts which are integrated forward in time using a second-order Runge-Kutta method in Matlab (R2019b; MathWorks, Natick, Massachusetts, USA). We scaled this model to 1,925 reef containing grid cells, identified by projecting the Millennium Coral Reef Mapping Project (https://data.unep-wcmc.org/datasets/1) map of corals reefs to the grid used by the NOAA Geophysical Fluid Dynamics Laboratory (GFDL) Earth System Model 2M (ESM2M)[65]. To validate co-existence of the coral morphotypes in the absence of an anthropogenic warming signal, we executed the model from 1861-2300 with no warming (Fig. S2). The model was then executed from 1861-2100 using bias corrected monthly SST output from ESM2M for each of the four representative concentration pathways (RCP) IPCC AR5 warming scenarios[16,65], using a time-step of 0.125 months. Combining a heuristic model, at the scale of a coral, with projected climate model resolution is justified based on the ability of coarse thermal stress data to predict the likelihood of bleaching[40]; this approach has been used in previous coral modelling studies[9,13–18]. All Matlab code can be found at https://github.com/VeloSteve/Coral-Model-V12 under the following DOI: https://doi.org/10.5281/zenodo.2639126.

Model output analysis (bleaching, mortality, and recovery definitions). For the purposes of visualizing model output for each model year, reef cells are categorized as being healthy, bleached or frequently bleached (≥2 events within the previous decade), or in a mortality state (Fig. S4). However, this heuristic model implementation is not intended to make absolute predictions of coral cover, bleaching, or mortality for individual reefs. Instead, it is calibrated to give zero mortality by 1950 and 3 or 5% bleaching per reef cell per year on average between 1985-2010. This approximation to actual conditions allows the model to represent the effect of alternate climate scenarios and other conditions. For these purposes, 'bleaching' events are defined by comparing the minimum annual symbiont density in each reef cell to the previous year. By defining bleaching events, we can compare the results to previous threshold based models[13,14,16,68]. Bleaching events herein are defined when symbiont density decreases below 30% of the minimum symbiont population size in the previous year, based on data showing that visible severe bleaching can occur even when corals retain between 20-50% of their original algal population[69]. This definition was developed to capture warm water bleaching events, but cold-water bleaching can occur[70]. Reef cells also enter a bleached state when bleaching occurs ≥2 times in the previous decade (similar to [13]). If either coral type bleaches in a given year, the reef cell enters a "bleached state". A single reef cell can only bleach once per year.

Following bleaching, a reef cell can remain bleached, transition to a state of mortality, or recover back to a 'healthy' state (Fig. S4). A mortality state is defined for a reef cell when a coral population declines below twice its seed value, regardless of symbiont density. A reef cell also enters a state of mortality if it does not recover within five years after bleaching. Although it is not

ecologically realistic for a reef to remain bleached for more than a few weeks to months, this categorization allowed us to differentiate between short- and long-term bleaching effects. To include the potential for recovery following bleaching or mortality, but in the absence of data to explicitly model connectivity between reefs globally, a small "seed" population of corals and symbionts is included at all time steps to represent resupply of larvae from source populations. For mounding and branching coral morphotypes, respectively, the seed population sizes are 1% and 0.1% of carrying capacity which assumes mounding (heat-tolerant) corals are 10 times more abundant than branching (heat-sensitive) corals following a bleaching or mortality event[49]. For symbionts, the seed density is 0.00001% of carrying capacity, calculated with the conservative assumption that coral population size is at its seed value. In model runs with evolution, seed symbionts are assumed to be adapted to temperature changes through time. For recovery to occur, both coral and symbiont populations must grow to at least four times their respective seed values. In addition, because coral growth can slowly increase despite fluctuations in symbiont population size, recovery is also defined when a coral population grows to >10% of carrying capacity.

Vulnerability maps based on warming rates and temperature variability. To compare predicted regions of vulnerability based on SST changes alone with model results, we produced maps based on temperature metrics expected to trigger bleaching and mortality (Fig S9). These maps included five metrics: change in maximum monthly mean SST from the historical period (1861-1900) to 2080, change in SST variability from the historical period (1861-1900) to the period between 2050-2080 (maximum monthly mean, all months), and future SST variability between 2050-2080 (maximum monthly mean, all months) for RCP4.5 and RCP8.5. To evaluate these metrics as possible predictors of modeled extinction risk, we also compared each metric to relative coral extent using a least-squares linear regression across all combinations of evolution and shuffling simulations. R^2 values were calculated each year between 2020-2060 using a sliding window for the future climatological period or year, for all reef cells containing >5% relative coral extent, and averaged over time. This timeframe maximized the number of reef cells that could be used in the analysis, prior to extensive degradation in all simulations (Fig. 1).

Acknowledgements

This work was supported by a NOAA Coral Reef Conservation grant to J.P.D. and S.D.D., a Coral Reef Alliance Coral Adaptation Challenge grant to C.A.L. and S.D.D., and an ROA supplement to NSF DEB #1655475 to C.A.L. and M.L.B. We thank C.M. Eakin for helpful initial discussions in the development of the global model. We are also grateful to four anonymous reviewers for valuable comments and suggestions that improved the manuscript. The contents in this manuscript are solely the opinions of the authors and do not constitute a statement of policy, decision, or position on behalf of NOAA or the US Government.

Code Availability

All Matlab code can be found at https://github.com/VeloSteve/Coral-Model-V12 under the following DOI: https://doi.org/10.5281/zenodo.2639126.

References

1. Poloczanska, E., Mintenbeck, K., Portner, H. O., Roberts, D. & Levin, L. A. *The IPCC Special Report on the Ocean and Cryosphere in a Changing Climate*. (2019).
2. Urban, M.C. Accelerating extinction risk from climate change. *Science* **348**, (2015).
3. McCauley, D. J. & Pinsky, M. L. Marine defaunation: animal loss in the global ocean. *Science* **347**, 1255641 (2015).
4. Hoffmann, A. A. & Sgrò, C. M. Climate change and evolutionary adaptation. *Nature* **470**, 479–485 (2011).
5. Somero, G. N. The physiology of climate change: how potentials for acclimatization and genetic adaptation will determine 'winners' and 'losers'. *J. Exp. Biol* **213**, 912–920 (2010).
6. Kearney, M. & Porter, W. Mechanistic niche modelling: combining physiological and spatial data to predict species' ranges. *Ecology Letters* **12**, 334–350 (2009).
7. Foden, W. B. *et al.* Identifying the world's most climate change vulnerable species: a systematic trait-based assessment of all birds, amphibians and corals. *PloS One* **8**, e65427 (2013).
8. West, J. M. & Salm, R. V. Resistance and resilience to coral bleaching: implications for coral reef conservation and management. *Conservation Biology* **17**, 956–967 (2003).
9. Baskett, M. L., Nisbet, R. M., Kappel, C. V., Mumby, P. J. & Gaines, S. D. Conservation management approaches to protecting the capacity for corals to respond to climate change: a theoretical comparison. *Global Change Biology* **16**, 1229–1246 (2010).
10. Beyer, H. L. *et al.* Risk-sensitive planning for conserving coral reefs under rapid climate change. *Conservation Letters* **11**, e12587 (2018).
11. Walsworth, T. E. *et al.* Management for network diversity speeds evolutionary adaptation to climate change. *Nature Climate Change* **9**, 632–636 (2019).
12. Hughes, T. P. *et al.* Spatial and temporal patterns of mass bleaching of corals in the Anthropocene. *Science* **359**, 80–83 (2018).
13. Donner, S. D., Skirving, W. J., Little, C. M., Oppenheimer, M. & Hoegh-Guldberg, O. Global assessment of coral bleaching and required rates of adaptation under climate change. *Global Change Biol* **11**, 2251–2265 (2005).
14. Frieler, K. *et al.* Limiting global warming to 2°C is unlikely to save most coral reefs. *Nature Climate Change* **3**, 165–170 (2012).
15. Van Hooidonk, R., Maynard, J. A., Manzello, D. & Planes, S. Opposite latitudinal gradients in projected ocean acidification and bleaching impacts on coral reefs. *Global Change Biology* **20**, 103–112 (2014).
16. Logan, C. A., Dunne, J. P., Eakin, C. M. & Donner, S. D. Incorporating adaptive responses into future projections of coral bleaching. *Global Change Biology* **20**, 125–139 (2014).
17. Bay, R. A., Rose, N. H., Logan, C. A. & Palumbi, S. R. Genomic models predict successful coral adaptation if future ocean warming rates are reduced. *Science Advances* **3**, e1701413 (2017).
18. Matz, M. V., Treml, E. A. & Haller, B. C. Estimating the potential for coral adaptation to global warming across the Indo-West Pacific. *Global Change Biology* **26**, 3473–3481 (2020).
19. Baskett, M. L., Gaines, S. D. & Nisbet, R. M. Symbiont diversity may help coral reefs survive moderate climate change. *Ecological Applications* **19**, 3–17 (2009).
20. Matz, M. V., Treml, E. A., Aglyamova, G. V. & Bay, L. K. Potential and limits for rapid genetic adaptation to warming in a Great Barrier Reef coral. *PLoS Genetics* **14**, e1007220 (2018).
21. Muscatine, L., Falkowski, P. G., Porter, J. W. & Dubinsky, Z. Fate of photosynthetic fixed carbon in light-and shade-adapted colonies of the symbiotic coral *Stylophora pistillata*. *Proceedings of the Royal Society of London. Series B. Biological Sciences* **222**, 181–202 (1984).
22. Csaszar, N. B., Ralph, P. J., Frankham, R., Berkelmans, R. & van Oppen, M. J. Estimating the potential for adaptation of corals to climate warming. *PLoS One* **5**, e9751 (2010).
23. Howells, E. J. *et al.* Coral thermal tolerance shaped by local adaptation of photosymbionts. *Nature Climate Change* **2**, 116 (2012).

24. Buerger, P. *et al.* Heat-evolved microalgal symbionts increase coral bleaching tolerance. *Science Advances* **6**, eaba2498 (2020).
25. Baker, A. C. Flexibility and specificity in coral-algal symbiosis: diversity, ecology, and biogeography of *Symbiodinium*. *Annual Review of Ecology, Evolution, and Systematics* 661–689 (2003).
26. Berkelmans, R. & van Oppen, M. J. H. van. The role of zooxanthellae in the thermal tolerance of corals: a 'nugget of hope' for coral reefs in an era of climate change. *Proc. R. Soc. B* **273**, 2305–2312 (2006).
27. National Academies of Sciences & Medicine. *A research review of interventions to increase the persistence and resilience of coral reefs*. (National Academies Press, 2019).
28. National Academies of Sciences. *A Decision Framework for Interventions to Increase the Persistence and Resilience of Coral Reefs*. (National Academies Press, 2019).
29. Darling, E. S., Alvarez-Filip, L., Oliver, T. A., McClanahan, T. R. & Côté, I. M. Evaluating life-history strategies of reef corals from species traits. *Ecology Letters* **15**, 1378–1386 (2012).
30. Chan, N. C. S. & Connolly, S. R. Sensitivity of coral calcification to ocean acidification: a meta-analysis. *Global Change Biology* **19**, 282–290 (2013).
31. Hughes, T. P. *et al.* Global warming transforms coral reef assemblages. *Nature* **556**, 492 (2018).
32. Darling, E. S. *et al.* Relationships between structural complexity, coral traits, and reef fish assemblages. *Coral Reefs* **36**, 561–575 (2017).
33. Howells, E. J. *et al.* Corals in the hottest reefs in the world exhibit symbiont fidelity not flexibility. *Molecular Ecology* **29**, 899–911 (2020).
34. Madin, J. S., Hughes, T. P. & Connolly, S. R. Calcification, storm damage and population resilience of tabular corals under climate change. *PLoS One* **7**, e46637 (2012).
35. Hoegh-Guldberg, O. *et al.* Impacts of 1.5 ºC global warming on natural and human systems. (2018).
36. Darling, E. S. *et al.* Social–environmental drivers inform strategic management of coral reefs in the Anthropocene. *Nature Ecology & Evolution* **3**, 1341–1350 (2019).
37. Wilkinson, C. R. Global and local threats to coral reef functioning and existence: review and predictions. *Mar. Freshwater Res.* **50**, 867–878 (1999).
38. Palumbi, S. R., Barshis, D. J., Traylor-Knowles, N. & Bay, R. A. Mechanisms of reef coral resistance to future climate change. *Science* **344**, 895–898 (2014).
39. Kleypas, J. A. *et al.* Larval connectivity across temperature gradients and its potential effect on heat tolerance in coral populations. *Global Change Biology* **22**, 3539–3549 (2016).
40. Heron, S. F. *et al.* Validation of reef-scale thermal stress satellite products for coral bleaching monitoring. *Remote Sensing* **8**, 59 (2016).
41. Safaie, A. *et al.* High frequency temperature variability reduces the risk of coral bleaching. *Nature Communications* **9**, 1–12 (2018).
42. Forster, P. M. *et al.* Evaluating adjusted forcing and model spread for historical and future scenarios in the CMIP5 generation of climate models. *Journal of Geophysical Research: Atmospheres* **118**, 1139–1150 (2013).
43. Ziegler, M. *et al.* Biogeography and molecular diversity of coral symbionts in the genus *Symbiodinium* around the Arabian Peninsula. *Journal of Biogeography* **44**, 674–686 (2017).
44. Sampayo, E. M., Ridgway, T., Bongaerts, P. & Hoegh-Guldberg, O. Bleaching susceptibility and mortality of corals are determined by fine-scale differences in symbiont type. *PNAS* **105**, 10444–10449 (2008).
45. Thornhill, D. J., Xiang, Y. U., Fitt, W. K. & Santos, S. R. Reef endemism, host specificity and temporal stability in populations of symbiotic dinoflagellates from two ecologically dominant Caribbean corals. *PLoS One* **4**, e6262 (2009).
46. Stat, M., Loh, W. K. W., LaJeunesse, T. C., Hoegh-Guldberg, O. & Carter, D. A. Stability of coral–endosymbiont associations during and after a thermal stress event in the southern Great Barrier Reef. *Coral Reefs* **28**, 709–713 (2009).
47. Chakravarti, L. J., Beltran, V. H. & van Oppen, M. J. Rapid thermal adaptation in photosymbionts of reef-building corals. *Global Change Biology* **23**, 4675–4688 (2017).
48. Schulte, P. M., Healy, T. M. & Fangue, N. A. Thermal performance curves, phenotypic plasticity, and the time scales of temperature exposure. *Integrative and Comparative Biology* **51**, 691–702 (2011).

Additional References in Online Methods

49. Loya, Y. *et al.* Coral bleaching: the winners and the losers. *Ecology Letters* **4**, 122–131 (2001).
50. Langmead, O. & Sheppard, C. Coral reef community dynamics and disturbance: a simulation model. *Ecological Modelling* **175**, 271–290 (2004).
51. Chancerelle, Y. Methods to estimate actual surface areas of scleractinian coral at the colony-and community-scale. *Oceanologica Acta* **23**, 211–219 (2000).
52. Falkowski, P. G., Dubinsky, Z., Muscatine, L. & Porter, J. W. Light and the bioenergetics of a symbiotic coral. *Bioscience* **34**, 705–709 (1984).
53. Huston, M. Variation in coral growth rates with depth at Discovery Bay, Jamaica. *Coral Reefs* **4**, 19–25 (1985).
54. Hoogenboom, M., Beraud, E. & Ferrier-Pagès, C. Relationship between symbiont density and photosynthetic carbon acquisition in the temperate coral *Cladocora caespitosa*. *Coral Reefs* **29**, 21–29 (2010).
55. Cunning, R. & Baker, A. C. Not just who, but how many: the importance of partner abundance in reef coral symbioses. *Frontiers in Microbiology* **5**, 400 (2014).
56. McClanahan, T., Muthiga, N. & Mangi, S. Coral and algal changes after the 1998 coral bleaching: interaction with reef management and herbivores on Kenyan reefs. *Coral Reefs* **19**, 380–391 (2001).
57. Fitt, W. K., McFarland, F. K., Warner, M. E. & Chilcoat, G. C. Seasonal patterns of tissue biomass and densities of symbiotic dinoflagellates in reef corals and relation to coral bleaching. *Limnology and Oceanography* **45**, 677–685 (2000).
58. Eppley, R. W. Temperature and phytoplankton growth in the sea. *Fish. Bull* **70**, 1063–1085 (1972).
59. Jon Norberg. Biodiversity and Ecosystem Functioning: A Complex Adaptive Systems Approach. *Limnology and Oceanography* **49**, 1269–1277 (2004).
60. Mousseau, T. A. & Roff, D. A. Natural selection and the heritability of fitness components. *Heredity* **59**, 181 (1987).
61. Lynch, M. The rate of polygenic mutation. *Genetics Research* **51**, 137–148 (1988).
62. Donner, S. D., Rickbeil, G. J. & Heron, S. F. A new, high-resolution global mass coral bleaching database. *PLoS One* **12**, e0175490 (2017).
63. Cunning, R., Gillette, P., Capo, T., Galvez, K. & Baker, A. C. Growth tradeoffs associated with thermotolerant symbionts in the coral *Pocillopora damicornis* are lost in warmer oceans. *Coral Reefs* **34**, 155–160 (2015).
64. Silverstein, R. N., Cunning, R. & Baker, A. C. Change in algal symbiont communities after bleaching, not prior heat exposure, increases heat tolerance of reef corals. *Global Change Biology* **21**, 236–249 (2015).
65. Dunne, J. P. *et al.* GFDL's ESM2 global coupled climate-carbon Earth System Models Part I: Physical formulation and baseline simulation characteristics. *J. Climate* **25**, 6646–6665 (2012).
66. Dunne, J. P. *et al.* GFDL's ESM2 Global Coupled Climate–Carbon Earth System Models. Part II: Carbon System Formulation and Baseline Simulation Characteristics. *J. Climate* **26**, 2247–2267 (2012).
67. Lough, J. M. & Barnes, D. J. Environmental controls on growth of the massive coral Porites. *Journal of Experimental Marine Biology and Ecology* **245**, 225–243 (2000).
68. van Hooidonk, R., Maynard, J. A. & Planes, S. Temporary refugia for coral reefs in a warming world. *Nature Clim. Change* **3**, 508–511 (2013).
69. Fitt, W., Brown, B., Warner, M. & Dunne, R. Coral bleaching: interpretation of thermal tolerance limits and thermal thresholds in tropical corals. *Coral Reefs* **20**, 51–65 (2001).
70. González-Espinosa, P. C., & Donner, S. D. Predicting cold-water bleaching in corals: role of temperature, and potential integration of light exposure. *Marine Ecology Progress Series*, **642**, 133-146 (2020).

Figures and Tables

Table 1. Global coral health metrics at 2100 in simulations with and without adaptive capacity. For each simulation and RCP, relative coral extent ("% Cover") reported as percent of a pre-warming fixed carrying capacity in each reef cell, percentage of reef cells not bleached or dead ("% Healthy"), and percentage of reef cells where branching (heat-sensitive) corals ("% Branching") are the dominant coral morphotype are reported. Color is associated with high (≥70%: blue-green), moderate (30-70%: yellow-orange), and low levels of each metric (≤30%: red-orange).

	No Adaptive Capacity			Symbiont Evolution			Symbiont Shuffling (+1°C)			Shuffling (+1°C) & Evolution		
RCP	% Cover	% Healthy	% Branching	% Cover	% Healthy	% Branching	% Cover	% Healthy	% Branching	% Cover	% Healthy	% Branching
2.6	37	57	2	81	84	61	65	85	56	72	96	71
4.5	3	5	0	41	71	18	28	65	20	65	94	62
6	1	1	0	7	21	0	5	21	1	58	90	57
8.5	1	0	0	1	0	0	1	0	0	10	23	13

Figures

Figure 1.

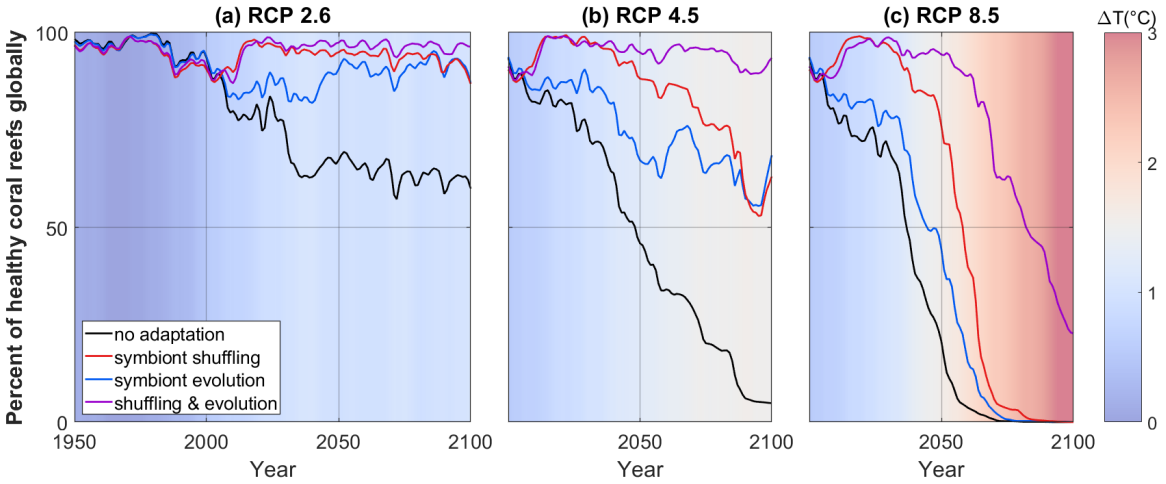

Figure 1. Percentage of 'healthy' reef cells globally in four RCP emissions scenarios from 1950-2100 (*n*=1,925 reef cells). Model trajectories are shown with no adaptation (black), symbiont shuffling with a +1°C advantage (red), symbiont evolution (blue), and combined shuffling and evolution (purple). A reef is considered 'healthy' if it is not in a bleached or mortality state (see *Methods*). Background color represents the average increase in annual maximum temperatures relative to the historical average from 1860 to 2000 across all reef grid cells.

Figure 2.

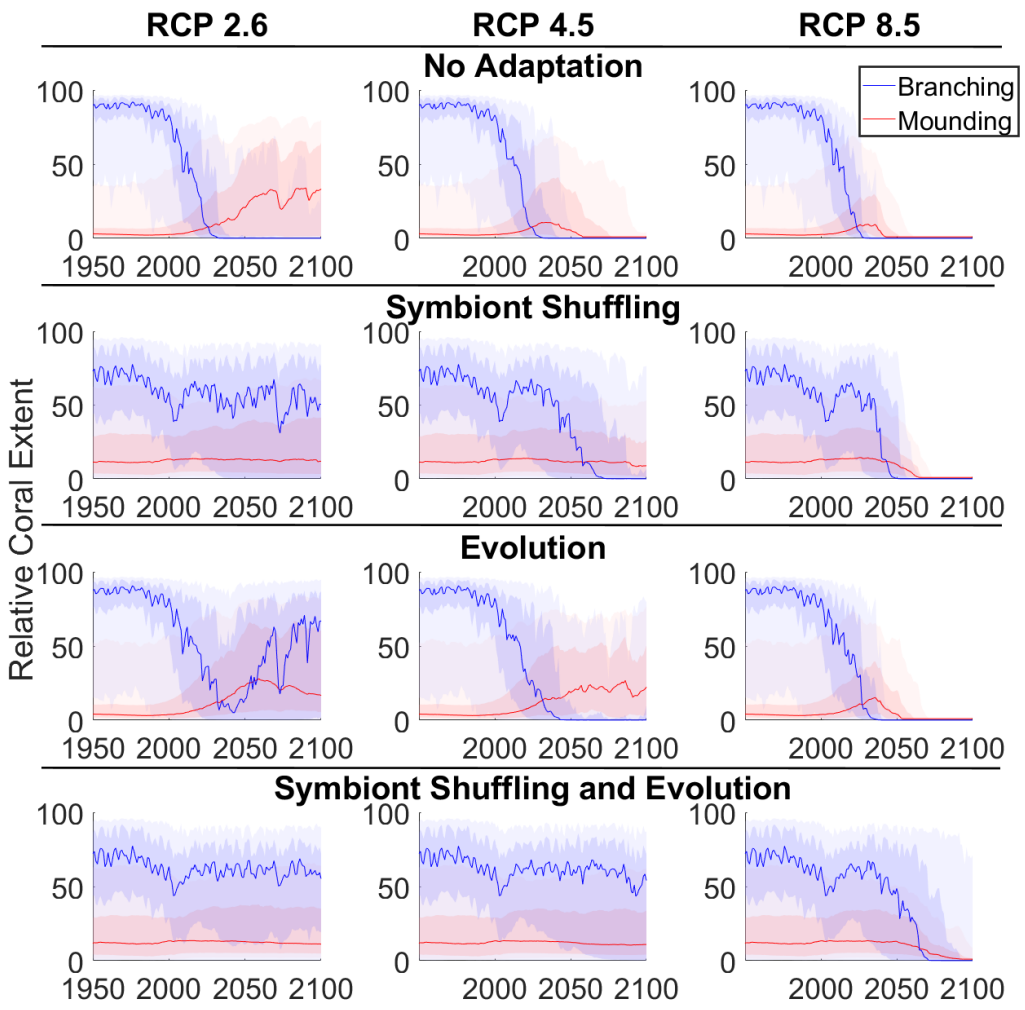

Figure 2. Relative coral extent with and without symbiont-mediated adaptive capacity. Mean, quartile, and 5th to 95th percentiles across all reef cells (n=1,925) for branching (heat-sensitive) corals and mounding (heat-tolerant) corals as a percent of a fixed pre-warming carrying capacity (K) averaged across all reef cells. Panels show simulations with no adaptation (top row), with symbiont shuffling only (+1°C advantage) (2nd row), with symbiont evolution only (3rd row), and combined shuffling and evolution (bottom row). Columns correspond to low (RCP2.6), moderate (RCP4.5), and high (RCP8.5) emissions scenarios.

Figure 3.

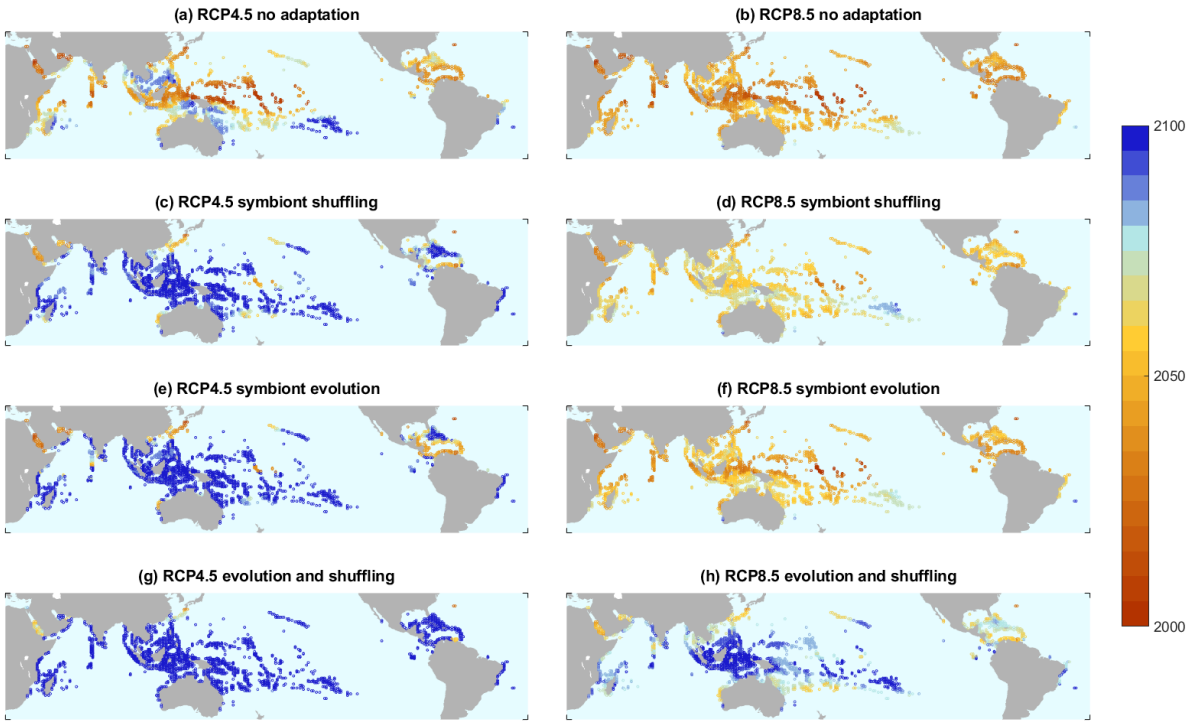

Figure 3. Maps depicting the last year at which corals are projected to survive prior to the onset of high frequency bleaching (≥2 events within the previous decade) or mortality. Model output is shown with no adaptation (a, b), symbiont shuffling with a +1°C advantage (c, d), symbiont evolution (e, f), or both shuffling and evolution (g, h) under moderate (RCP 4.5) and high (RCP8.5) emissions scenarios. Reef cells in the darkest blue are projected to survive beyond 2100.

Supplemental Tables

Table S1

	No Adaptive Capacity			Symbiont Evolution Only			*Symbiont Shuffling Only*									*Symbiont Shuffling & Evolution*								
							+0.5°C			+1.0°C			+1.5°C			+0.5°C			+1.0°C			+1.5°C		
RCP	% Cover	% Healthy	% Sensitive	% Cover	% Healthy	% Sensitive	% Cover	% Healthy	% Sensitive	% Cover	% Healthy	% Sensitive	% Cover	% Healthy	% Sensitive	% Cover	% Healthy	% Sensitive	% Cover	% Healthy	% Sensitive	% Cover	% Healthy	% Sensitive
2.6	37	57	2	81	84	61	30	50	11	65	85	56	77	96	86	58	79	47	72	96	71	76	96	84
4.5	3	5	0	41	71	18	2	3	0	28	65	20	76	97	76	38	62	29	65	94	62	72	96	80
6	1	1	0	7	21	0	1	0	0	5	21	1	58	91	62	18	40	16	58	90	57	73	98	73
8.5	1	0	0	1	0	0	1	0	0	1	0	0	3	8	1	1	0	0	10	23	13	47	86	5

Table S1. Global coral health metrics at 2100 in simulations with and without adaptive capacity. For each simulation and RCP, relative coral extent ("% Cover") reported as percent of a pre-warming fixed carrying capacity in each reef cell, percentage of reef cells not bleached or dead ("% Healthy"), and percentage of reef cells where branching (heat-sensitive) corals ("% Branching") are the dominant coral morphotype are reported. Color is associated with high (≥70%: blue-green), moderate (30-70%: yellow-orange), and low levels of each metric (≤30%: red-orange). For shuffling, the heat-tolerant symbiont population thermal optimum is +0.5°C, +1.0°C, or +1.5°C greater than the heat-sensitive population.

Table S2.

Parameter	Value	Units	Description	Reference
Corals				
K_{Cm}	m: 7.4125; b: 10.25	X 10^7 cm^2	coral carrying capacity	Chancerelle (2000); Mumby (2006)
α	m: 0.75; b: 0.85		competition coefficient	Langmead and Sheppard (2004)
γ	m: 1; b: 10	yr^{-1}	growth rate	Huston (1985)
μ	m: 3.849; b: 58.767	X 10^2 yr^{-1}	basal mortality	Chancerelle (2000); McClanahan et al. (2001)
u	m: 20,000; b: 30,000		symbiont influence on mortality	Fitt et al. (2000)
Symbionts				
K_{Sm}	m: 3; b: 4	X 10^6 cells/cm^2	symbiont carrying capacity	Fitt et al. (2000)
a	1.0768	yr^{-1}	linear growth rate	Muscatine et al. (1984)
b	0.0633	C^{-1}	exponential growth constant	Norberg (2004); Eppley (1972)
σ^2_e	0.0114	$^oC^2$	environmental variance	Mousseau & Roff 1987; Csaszar et al 2010
σ^2_M	1.142	X 10^{-5} $^oC^2$ yr^{-1}	mutational variance	Lynch (1988); Muscatine et al. (1984)
σ^2_{wm}	m: 2.7702; b: 3.4627	$^oC^2$	selectional variance	Baskett et al. 2009
h^2	0.33		heritability	Mousseau & Roff 1987; Csaszar et al 2010

Table S2. Parameter values used in the numerical analysis of the model, adapted from Baskett et al. 2009 and references therein. m denotes values for mounding corals (heat-tolerant, slow growing) and b denotes those for branching corals (heat-sensitive, fast-growing). Symbiont carrying capacity (K_{Sm}) and selectional variance ($\sigma^2_{\omega m}$) vary depending on whether the symbionts inhabit a mounding (m) or branching coral (b).

Table S3

Symbiont assumptions	Proportionality constant divisor	
	no evolution	with evolution
Baseline	3.0446	3.2988
Shuffling, 0.5 °C	4.3923	4.8325
Shuffling, +1°C	4.1842	4.1986
Shuffling, +1.5 °C	3.3651	3.5697

Table S3. Proportionality constant divisor (*s*) in the proportionality constant equation (see *Methods*). Values were determined empirically to obtain a 5% global bleaching frequency between 1985 and 2010 (i.e., 5% of reef cells bleach each year, on average, during this timeframe). Each set of assumptions which affects historical growth requires a unique *s* value.

Table S4

	No Adaptation		Shuffling (1C)		Evolution		Shuffling + Evolution	
SST Metric	RCP4.5	RCP8.5	RCP4.5	RCP8.5	RCP4.5	RCP8.5	RCP 4.5	RCP 8.5
Hottest Month Delta SST Historical to Future Year	0.10	0.16	0.09	0.12	0.10	0.11	0.07	0.11
Hottest Month Delta std[SST] Historical to Future Climatology	0.06	0.02	0.03	0.06	0.09	0.04	0.04	0.05
Hottest Month std[SST] Future Climatology	0.08	0.06	0.06	0.11	0.12	0.10	0.03	0.06
All months Delta std[SST] Historical to Future Climatology	0.05	0.03	0.07	0.04	0.07	0.02	0.08	0.09
All months std[SST] Future Climatology	0.04	0.09	0.54	0.41	0.01	0.03	0.48	0.55

Table S4. Correlation (R^2) between relative coral extent and environmental SST metrics of warming rate and SST standard deviation for RCP4.5 and RCP8.5. A least-squares linear regression was used for all reef cells with >5% relative coral extent in each model simulation. Regression analysis was performed at each year between 2020-2060 using a sliding window for the future year or a 20-year future climatology ending in the analysis year, and averaged over time. The historical climatological period is calculated between 1861-1900.

Supplemental Figures

Figure S1

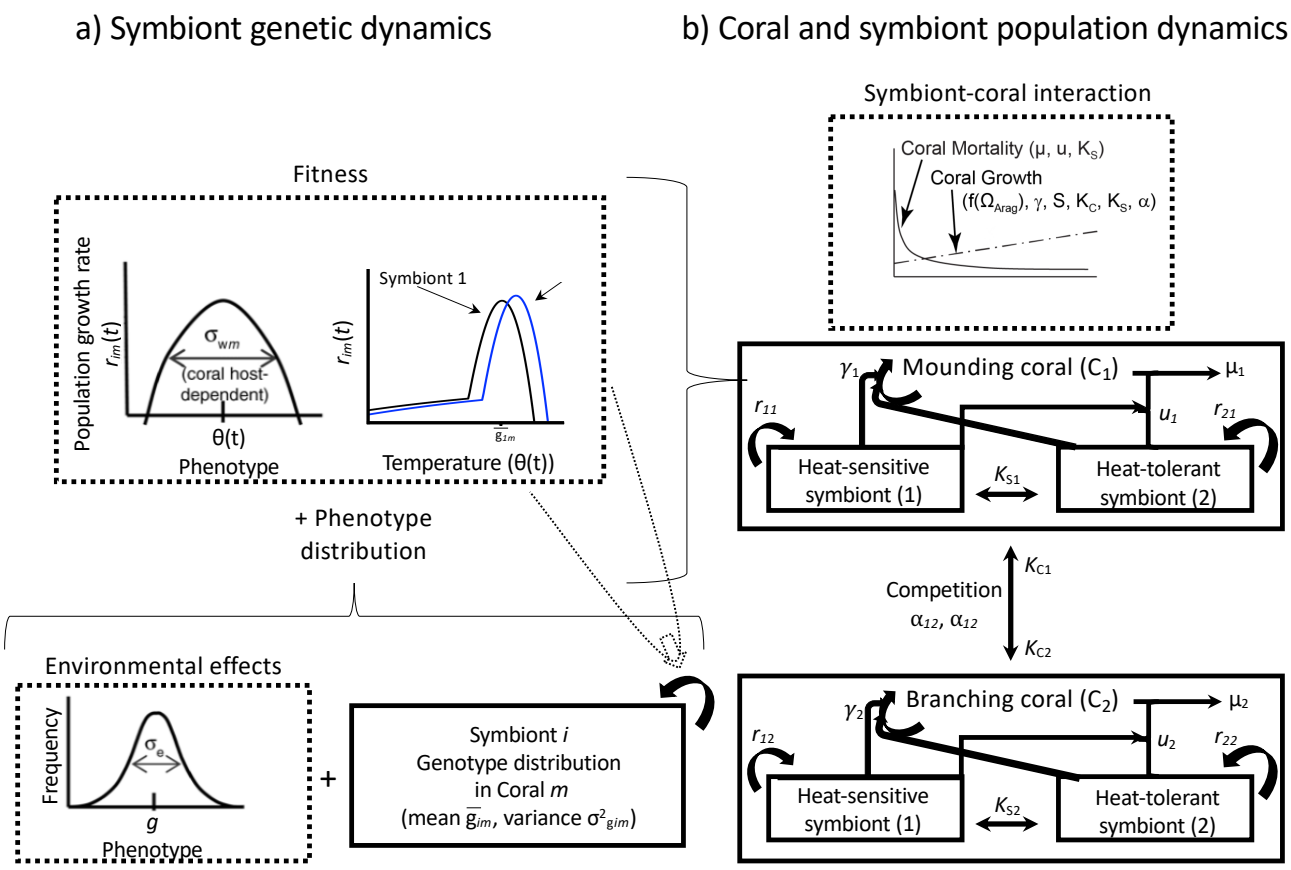

Differential Equations

(1) Coral population dynamics.

$$\frac{dC_m}{dt} = C_m\left[\frac{f^2\gamma_m \frac{\sum_i S_{im}}{K_{Sm}C_m}}{K_{Cm}}\left(K_{Cm} - \sum_n \alpha_{mn}C_n\right) - \frac{\mu_m}{1 + u_m\frac{\sum_i S_{im}}{K_{Sm}C_m}}\right]$$

(2) Symbiont population dynamics.

$$\frac{dS_{im}}{dt} = \frac{S_{im}}{K_{Sm}C_m}\left[r_{im}(t)K_{Sm}C_m - \hat{r}(t)\sum_j S_{jm}\right]$$

(3) Symbiont population growth rate. In shuffling model runs, $\bar{g}_{im}$ of the heat-tolerant symbiont population is set to +0.5, 1, or 1.5°C above that of the heat-sensitive population. L represents $\sqrt{2.6\sigma^2_{wm}}$.

$$r_{im}(t) = \left\{1 - \frac{\sigma^2_{gim}(t) + \sigma^2_e + [\min(L, \bar{g}_{im}(t) - \theta(t))]^2}{2\sigma^2_{wm}}\right\} a e^{b[\theta(t) - 2*\min(0, \theta(t) - \bar{g}_{im}(t) + L)]}$$

(4) Symbiont mean genotype (optimum temperature) dynamics (*for evolution model runs only*).

$$\frac{d\bar{g}_{im}}{dt} = \frac{\sigma^2_{gim}(t)[\theta(t) - \bar{g}_{im}(t)]}{\sigma^2_{wm}} ae^{b\theta(t)}$$

(5) Symbiont genetic variance dynamics (*for evolution model runs only*).

$$\frac{d\sigma^2_{gim}}{dt} = \sigma^2_M - \frac{\sigma^4_{gim}(t)}{\sigma^2_{wm}} ae^{b\theta(t)}$$

(6) Aragonite saturation effect (*for ocean acidification model runs only*).

$$f(\Omega_{Arag}) = 1 - 0.15(4 - \Omega_{Arag}) \;\; where \;\; 1 \leq \Omega_{Arag} \leq 4$$

Figure S1. Coral and symbiont ecological and evolutionary global model diagram and equations. The left-hand boxes (a) describe the symbiont fitness curve and genetic dynamics. The right-hand boxes (b) describe the coral and symbiont population dynamics.

Figure S2.

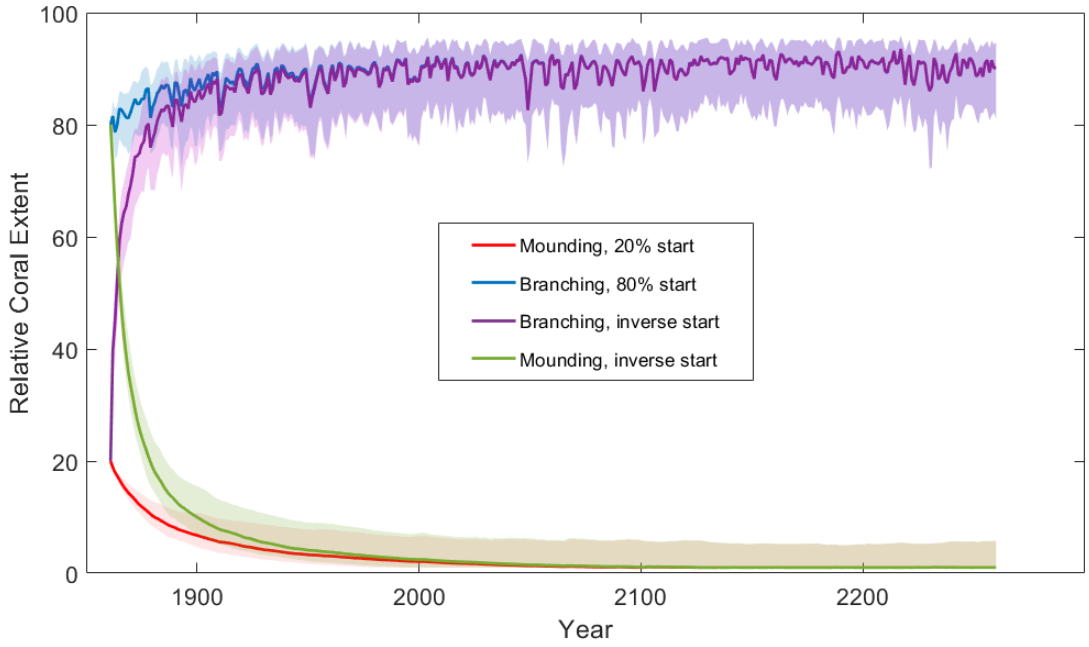

Figure S2. Relative coral extent across all reef cells in a 400-year model run with no anthropogenic warming and no adaptive capacity. In all model runs, branching corals (blue) are initialized at 80% and mounding corals (red) at 20% of a fixed pre-warming carrying capacity (K) in 1861 averaged across all reef cells. Initializing coral morphotypes to the inverse of these proportions (80% mounding: 20% branching) results in a similar outcome (~ 90% branching and 1% mounding corals) by 1950. Shaded colors represent the 50% interquartile range around the mean for all reef cells.

Figure S3.

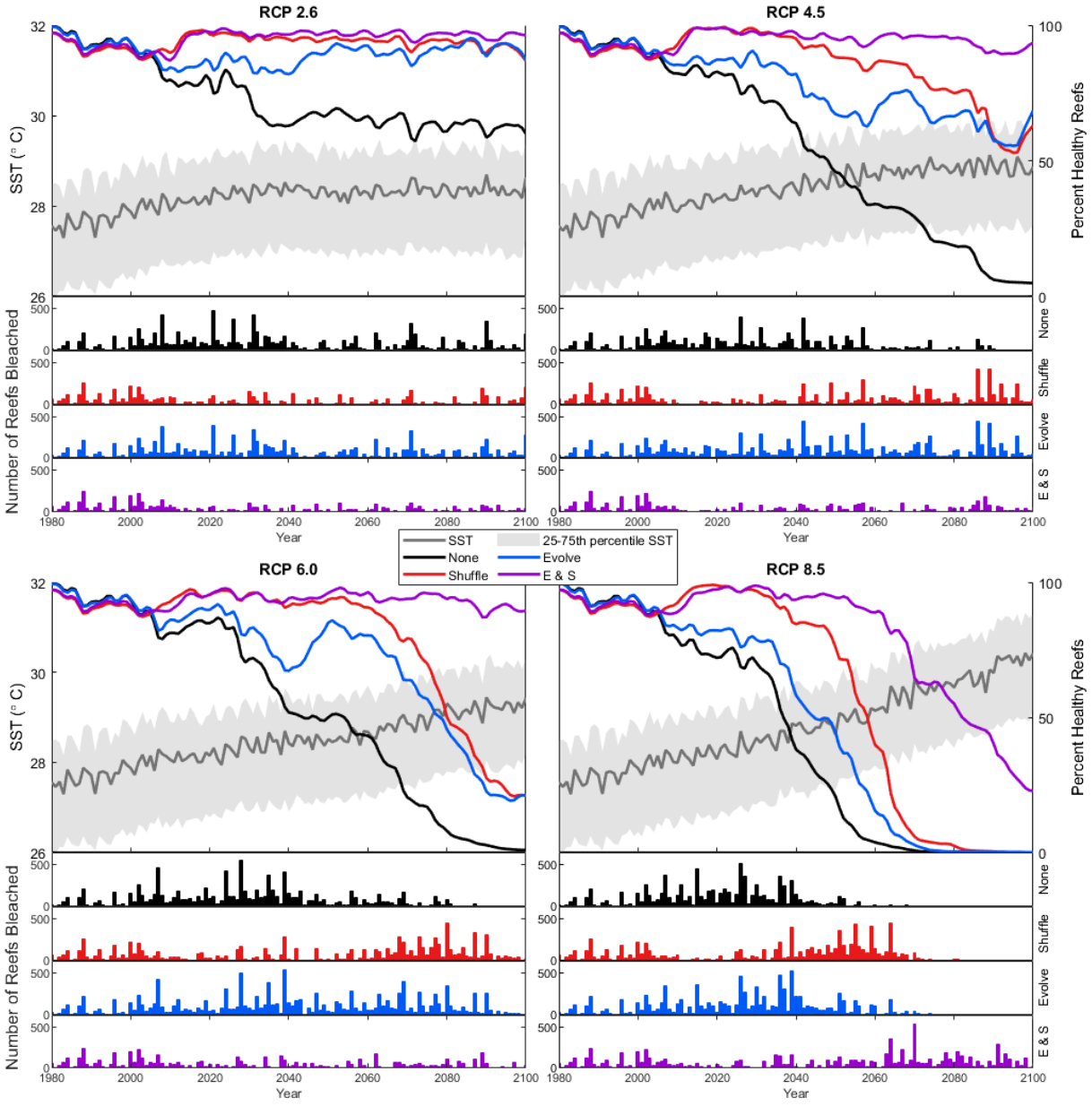

Figure S3. Percentage of 'healthy' reef cells globally in four RCP emissions scenarios from 1950 to 2100 (n=1,925 reef cells). Model trajectories are shown with no evolution (black), shuffling with a +1°C advantage (red), evolution (blue), and combined shuffling and evolution (purple). A reef is considered 'healthy' if it is not in a bleached or mortality state (see *Methods*). SST (grey) is the mean and 25th-75th percentile increase in annual maximum temperatures across all reef grid cells. Bar plots indicate number of bleaching events per year in each model run.

Figure S4.

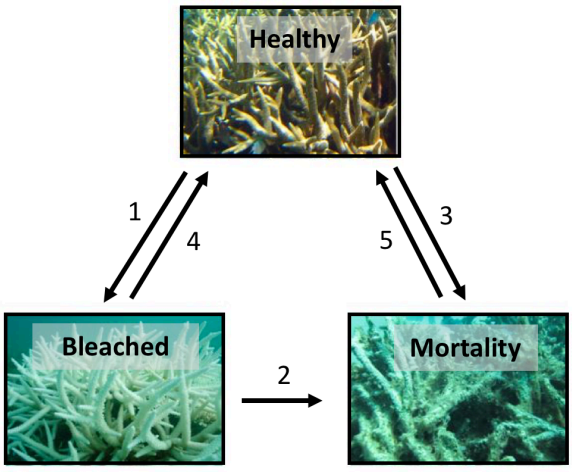

Figure S4. In each model year, reef cells are defined as being in a 'healthy', 'bleached', or 'mortality' state. Arrows represent transitions between states. 1) "Bleaching" occurs when symbiont populations drop <30% of the minimum population size in the previous year or when bleaching occurs ≥2 times in the previous decade. 2) "Mortality" is defined if a reef bleaches but does not recover within five years, or 3) if coral populations drop to <2x the seed value. 4-5) Recovery occurs if coral and symbiont populations increase to >4x their respective seed value or coral populations grow above 10% of carrying capacity.

Figure S5.

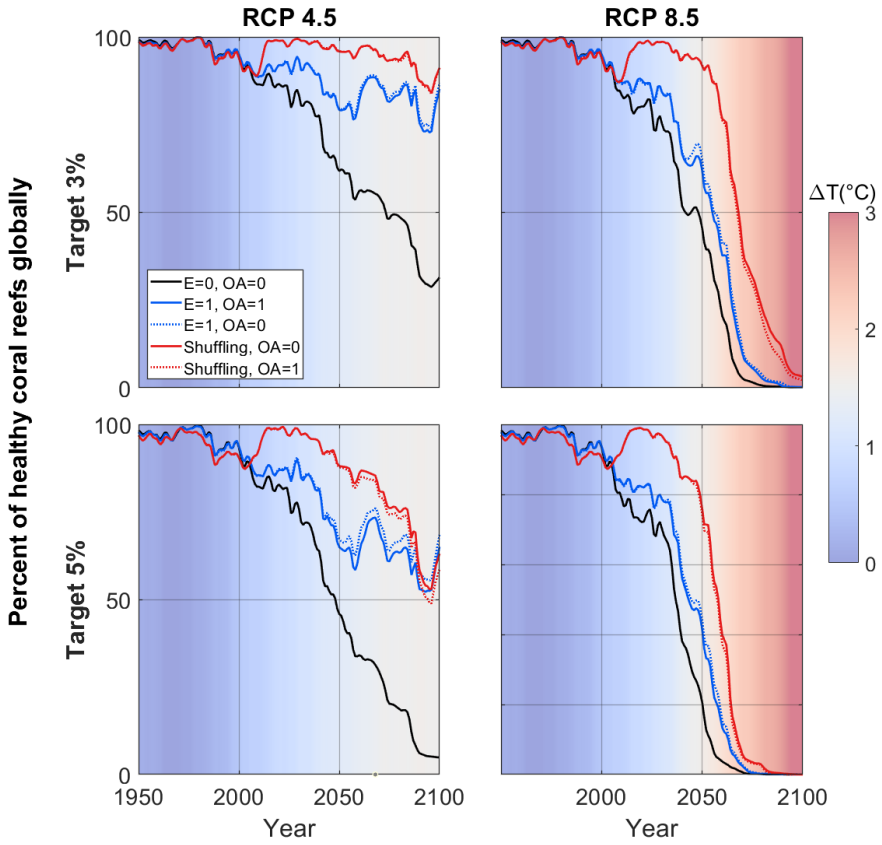

Figure S5. Sensitivity analysis of percent 'healthy' coral reef cells when the model is calibrated to estimated bleaching frequencies of 3 or 5% between 1985-2010. In the main text, model output is calibrated to a 5% bleaching frequency during this time. The effect of changing the target to 3 % is shown for RCP4.5 and RCP8.5 scenarios. Projected trajectories are shown with and without symbiont evolution (E=1 vs. E=0), and with or without shuffling (+1.0°C advantage) in the tolerant population. The effect of increasing pCO_2 on coral growth rates is also included (OA=1) with evolution and shuffling.

Figure S6

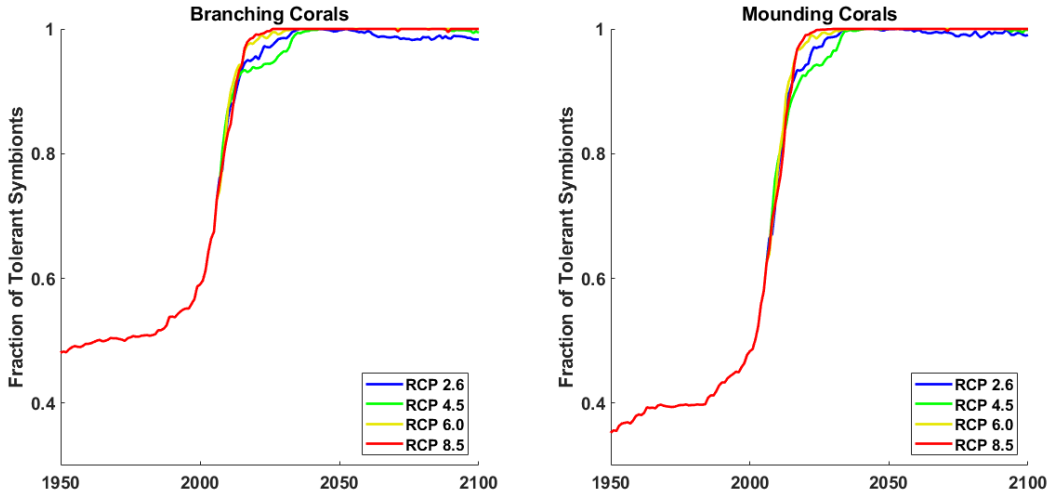

Figure S6. Global mean fraction of corals hosting heat-tolerant symbionts in branching (heat-sensitive) corals (left) and mounding (heat-tolerant) corals (right) across all reef cells (n=1,925) for all RCPs in shuffling (+1.0°C advantage) simulations. For most reefs, fidelity to heat-tolerant symbiont occurs following a rapid transition between 2010-2040 through 2100.

Figure S7

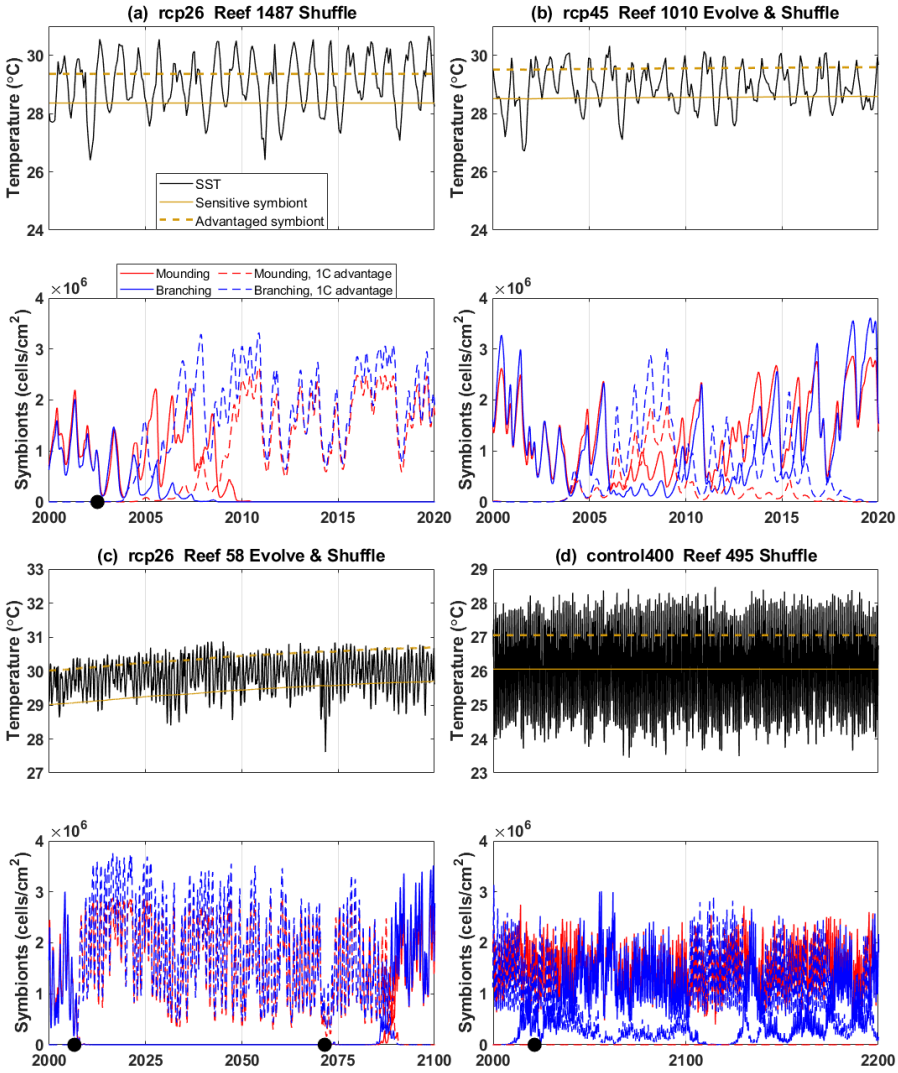

Figure S7. Fine-scale shuffling dynamics in four example reef cells. Temperature is monthly sea surface temperature (SST) with the optimal temperature (gi) for each symbiont type overlaid in yellow (top). Symbiont density (bottom) is in terms of cells per cm^2 of coral area for a heat-sensitive and heat-tolerant symbiont population in each coral morphotype. Realistic seasonal fluctuations in symbiont density (a,b) and reversion can occur (c, d), but reversion is uncommon under future RCP scenarios. (d) represents a no anthropogenic warming model run in which reversion occurs several times during a 200-year period. Bleaching events are shown in black circles.

Figure S8.

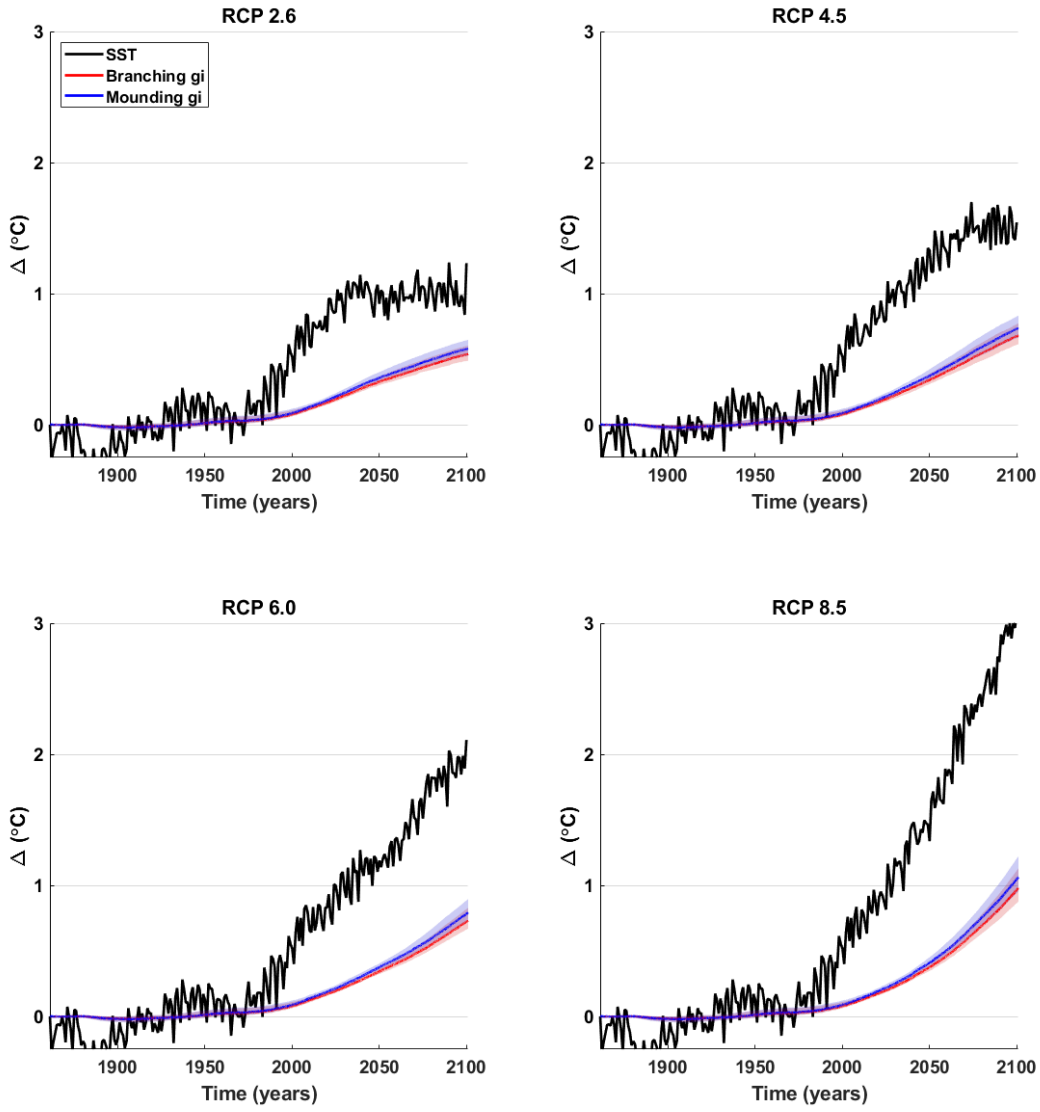

Figure S8. Global change in symbiont genotype (g_i or optimal temperature in °C) and average increase in annual maximum sea surface temperatures (SST) across all reef grid cells in model runs with symbiont evolution for all RCPs. Median (solid lines) and interquartile range (shaded) is shown across all reef cells (n=1,925) for mounding (heat-tolerant) and branching (heat-sensitive) corals. Across all RCP scenarios and all reefs, the increase in symbiont optimal thermal tolerance ranged between 0.3°C and 1.8°C.

Figure S9.

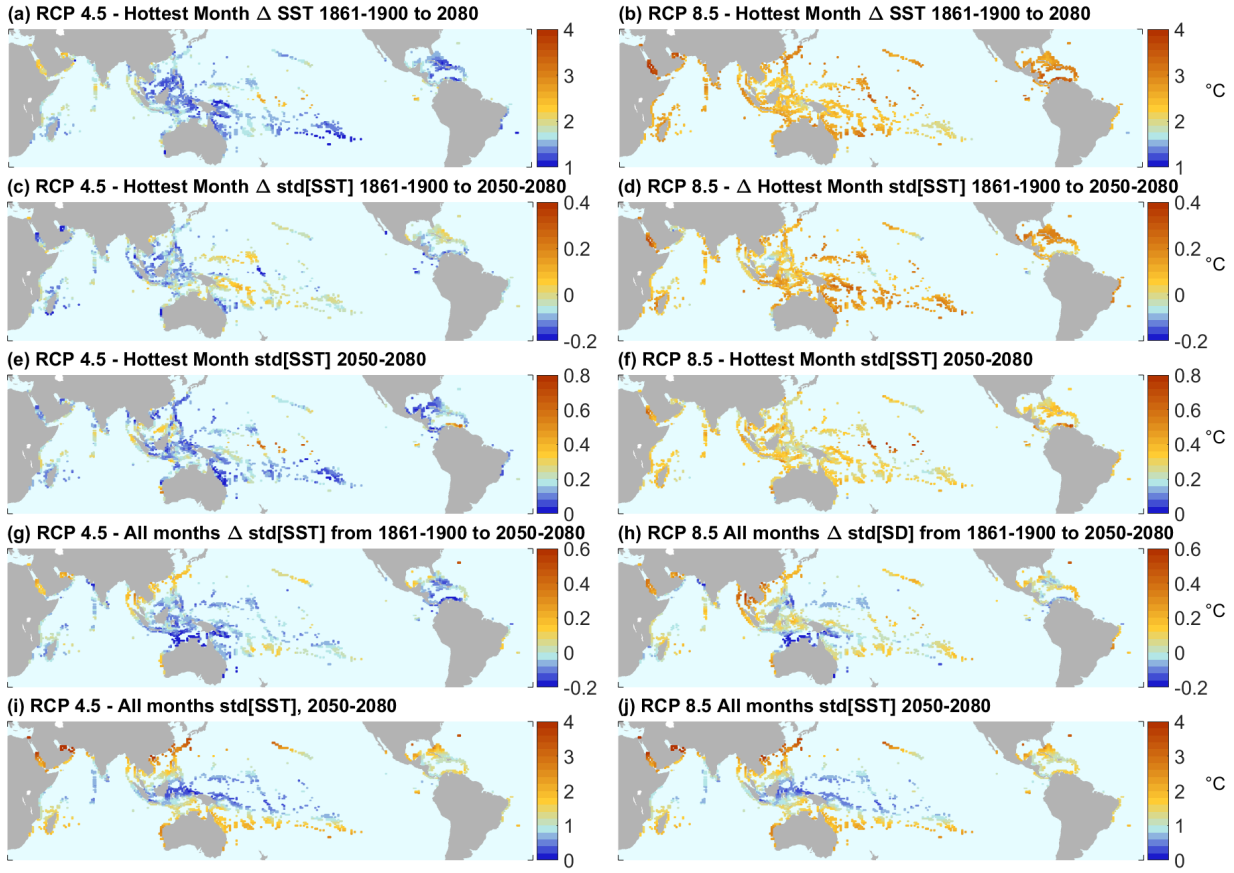

Figure S9. Global maps of warming rate and SST variability between the historical period (1861-1900) and 2080 (a-d, g-h) as well as future variability between 2050-2080 (e-f, i-j) for RCP 4.5 and RCP 8.5 climate scenarios. In panels (a) to (f), inputs are filtered to include only maximum monthly mean SST. Panels (g) through (j) include all months.